Title: Gestational psychedelic exposure disrupts brain development and offspring behavior in mice

Authors: Ya'el Courtney[1,2], Josephine M. Anderson[3], Christian Lagares-Linares[1,2], Cody J. Wenthur[3,4], Maria K. Lehtinen[1,2]*

Affiliations:

[1] Department of Pathology, Boston Children's Hospital and Harvard Medical School; Boston, MA, USA.
[2] Program in Neuroscience, Harvard Medical School; Boston, MA, USA.
[3] School of Pharmacy, University of Wisconsin; Madison, WI, USA.
[4] Transdisciplinary Center for Research in Psychoactive Substances, University of Wisconsin; Madison, WI, USA.

*Corresponding author. Email: maria.lehtinen@childrens.harvard.edu

Abstract: Despite increasing non-medical use and clinical investigation of psychedelics, the consequences of prenatal exposure remain unknown. In mice, maternal lysergic acid diethylamide (LSD; 0.3 mg kg^{-1}) crossed the placenta, appearing in embryonic cerebrospinal fluid (CSF) within minutes at E12.5 and E16.5. Within 30 minutes, LSD and other serotonergic psychedelics induced a 5-HT_2C agonist-like response in the choroid plexus, triggering apical remodeling and increasing CSF protein. A single E12.5 exposure altered cerebral cortical laminar organization and composition at postnatal day 8, and repeated dosing (E12.5–E16.5) amplified male-biased shifts from $SATB2^+$ to $CTIP2^+$ neuronal identities and increased microglia. Adult offspring showed reduced prepulse inhibition (male-predominant) and rotational stereotypy. These data identify an embryo-facing interface that detects maternal psychedelics and link CSF access to enduring neurodevelopmental and behavioral consequences.

Main Text:

The global resurgence of psychedelics in clinical research has sparked hope for treating intractable psychiatric conditions, including depression, PTSD, and addiction (*1*, *2*). As these compounds move toward mainstream therapeutic application, and as their non-clinical use reaches all-time highs, key questions remain about their safety in vulnerable populations, including during pregnancy. Despite widespread serotonergic signaling in the developing brain (*3–5*), the effects of maternal psychedelic exposure on fetal neurodevelopment remain virtually unexamined.

One candidate pathway through which psychedelics may influence fetal brain development is the choroid plexus (ChP)-cerebrospinal fluid (CSF system). The ChP is a secretory epithelium that produces CSF (*6*) and expresses 5-HT_2C (encoded by *HTR2C*) as its dominant serotonin receptor (*7*). In humans, *HTR2C* is detectable in ChP from both the lateral and fourth ventricles by ~6 weeks post-conception (~8 gestational weeks), a first-trimester stage when the plexus is forming and CSF cues begin to influence cortical development (*8*). The ChP plays a pivotal role in shaping the neurodevelopmental milieu during cerebral cortical neurogenesis (*9*). Our recent work demonstrated that maternal lysergic acid diethylamide (LSD) exposure perturbs gene expression in the embryonic ChP (*10*). Furthermore, we have shown that direct 5-HT_2C agonism with compounds like WAY-161503 is sufficient to alter CSF composition and disrupt cerebral cortical development, establishing this route as one plausible mechanism for serotonergic drug action. These findings raise the critical possibility that maternally administered psychedelics including LSD can access and disrupt this specialized brain barrier niche, with direct consequences for cerebral cortical development.

Here, we investigate how maternal exposure to LSD, a prototypical serotonergic psychedelic, affects fetal brain development in mice. Using in utero sampling and mass spectrometry, we show that LSD rapidly crosses the placenta and accumulates in embryonic CSF at both embryonic day (E) E12.5 and E16.5, with peak concentrations occurring approximately 15 minutes following injection. A single maternal dose at E12.5 disrupts excitatory neuron layering and glial development, while repeated exposure across five days exacerbates these effects. We also find that LSD activates the embryonic ChP and increases total CSF protein content, consistent with apocrine secretion into the ventricular system. Finally, mice exposed in utero exhibit long-lasting behavioral alterations as adults, including impaired sensorimotor gating and increased spontaneous locomotion. Together, these findings reveal that maternally administered psychedelics are capable of rapidly accessing and perturbing key embryonic signaling systems including the ChP-CSF nexus, underscoring the need for caution and further investigation as these compounds move into broader use.

Maternal LSD rapidly reaches embryonic CSF in mouse

To test whether maternally administered LSD reaches the embryo, we measured drug levels in maternal serum, embryonic serum (E16.5), and embryonic CSF at E12.5 and E16.5 following a single subcutaneous dose of 0.3 mg kg^{-1}; samples were collected at 5, 15, 30, 60, and 120 min (**Fig. 1A**). Doses were selected to ensure target engagement in mouse and are not human-equivalent. Maternal serum was obtained via cardiac puncture. At E16.5, embryonic serum was collected by venipuncture of a cervical vein under stereomicroscopic guidance using a pulled glass microcapillary pipette. Embryonic CSF was collected at E12.5 and E16.5 from the cisterna magna

using a glass microcapillary pipette under stereomicroscopic guidance, as previously described (*11*), minimizing blood or neuroepithelial contamination.

We developed a small-volume LC–MS/MS assay for mouse serum and embryonic CSF using d3-LSD as the internal standard. Calibration curves were prepared in-matrix (blank serum or artificial CSF), were linear across the working range ($R^2 \approx 0.997$), and supported a lower limit of quantitation of 0.25 ng mL^{-1}. Calibration curves prepared in-matrix met acceptance criteria, with back-calculated bias within −8% to +9% (serum) and −8% to +8% (CSF) and replicate CV ≤ 2.7% both matrices (**Fig. 1B–C**).

Following a single maternal dose of 0.3 mg kg^{-1}, maternal serum reached its highest concentration at 5 min (419.6 ng mL^{-1}) and then declined with an elimination half-life of ≈39.0 min based on the 30–120 min log-linear phase (**Fig. 1D**). At E16.5, embryonic serum peaked at 5 min (≈107.8 ng mL^{-1}; ~26% of the maternal maximum) and showed a half-life of ≈53.0 min by the same approach (**Fig. 1E**). Embryonic CSF contained measurable LSD by 5–15 min at both ages, with 15-min peaks of ≈15.2 ng mL^{-1} (E12.5; $t_{1/2}$ ≈64.9 min) and ≈28.4 ng mL^{-1} (E16.5; $t_{1/2}$ ≈52.5 min), remaining above the assay limit at 120 min (≈1.8 and 1.6 ng mL^{-1}, respectively) (**Fig. 1F**). At 15 min, CSF levels at E16.5 were ~1.9× those at E12.5 and were ~50% of the paired embryonic-serum concentration. Across 0–120 min, total embryonic-serum exposure was ~17% of maternal serum, and CSF exposure at E16.5 exceeded E12.5 by ~1.4×. These data indicate that LSD crosses the placenta and reaches the embryonic CSF within minutes; the longer CSF half-lives identify a window during which neural precursor cell targets may be exposed.

Prenatal LSD reshapes S1 neuron composition and microglia at P8

Maternal LSD perturbed S1 cerebral corticogenesis in a dose-dependent and partly sex-dependent manner (**Fig. 2**). The experimental design (**Fig. 2A**) contrasted a single 0.3 mg kg^{-1} injection at E12.5 ("acute") with the same dose given once daily from E12.5-E16.5 ("repeated"). At the 0.3 mg kg^{-1} dose, no adverse events such as maternal weight loss, altered grooming, or changes in pup retrieval were observed. Litter size, pup viability, birth weight, brain weight, and brain-to-body ratio at birth did not differ between LSD-exposed and control litters (**Fig. S1A-D**). Brains were examined at postnatal day 8 (P8), when laminar identities and glial profiles are well resolved but before extensive synaptic pruning.

Across six equal-width bins spanning pia to white matter, $DAPI^+$ nuclei were reduced following LSD (two-way ANOVA, Treatment effect $P < 0.0001$; **Fig. 2B**). Acute exposure produced the larger deficit, 1,090-2,020 cells mm^{-2} (21–49 % below control, post hoc $P \leq 0.0008$ in every bin), whereas repeated exposure reduced nuclei by 580 – 1,260 cells mm^{-2} (16–40 %; $P \leq 0.027$). A Treatment × Sex interaction was not detected for total nuclei ($F_{2,168} = 0.34$, $P = 0.71$), indicating a comparable global loss in males and females.

Cerebral cortical layer marker quantification revealed shifts among corticofugal ($CTIP2^+$), callosal ($SATB2^+$) and corticothalamic ($TBR1^+$) neurons (**Fig. 2C-E**). Repeated dosing increased the $CTIP2^+$ fraction from 19.7 ± 1.5 % to 28.1 ± 1.9 % (difference +8.4 percentage points [pp], Fisher's least significant difference post hoc $P = 0.026$), whereas acute dosing did not change $CTIP2^+$ abundance. $SATB2^+$ neurons were selectively vulnerable, dropping by 13.6 pp with repeated exposure (46.5 ± 1.6 % → 32.9 ± 2.1 %, $P < 0.0001$) and by 22.9 pp after acute exposure (to 23.7 ± 1.7 %, $P < 0.0001$). $TBR1^+$ neurons declined under both regimens (–12.8 pp repeated, –16.1 pp acute; $P \leq 0.0005$). The "DAPI-only" fraction (nuclei lacking these three markers) rose by 9.7 pp with repeated LSD ($P = 0.023$) and by 15.4 pp with acute LSD ($P = 0.0002$).

Stratifying by sex and cortical depth (**Fig. 2F–N**) revealed a significant Treatment × Sex × Bin interaction for CTIP2$^+$ and SATB2$^+$ populations ($F_{10,250} = 3.21$, $P = 0.0007$). In males, repeated LSD reduced SATB2$^+$ neurons in bins 1–5 by 28–52 % (all $P \leq 0.040$) and doubled CTIP2$^+$ neurons in bin 2 (+20.5 pp, $P = 0.0042$), with smaller gains in bin 5. Females showed no detectable CTIP2$^+$/SATB2$^+$ shifts. TBR1$^+$ loss was equivalent across sexes and confined to deep bins 5–6 (–19 – 22 pp; $P < 0.0001$). Acute exposure produced parallel SATB2$^+$ and TBR1$^+$ deficits in both sexes without altering CTIP2$^+$ levels.

IBA1$^+$ microglia density increased with repeated dosing from 166.8 ± 6.2 to 204.5 ± 8.3 cells mm^{-2} (+22 %, Dunnett post hoc $P = 0.0036$, **Fig. 2O**) and rose modestly after acute dosing (192.6 ± 9.8 cells mm^{-2}, +16 %, $P = 0.044$, **Fig. 2P**). GFAP staining revealed reactive astrocytic rims surrounding ectopic parvalbumin-positive interneuron clusters posterior to the anterior commissure, which only appeared in LSD-exposed mice (**Fig. S1E**).

In sum, prenatal LSD reduced S1 cellularity and shifted excitatory neuron identities at P8, with selective losses of SATB2$^+$ and TBR1$^+$ neurons under both regimens. Repeated dosing increased CTIP2$^+$ neurons. Effects varied by depth and were stronger in males. Microglial density increased, and astrocytic rims surrounded ectopic parvalbumin-positive clusters. These early cortical and glial signatures raise the hypothesis that prenatal exposure produces lasting functional changes in behavior.

Prenatal LSD exposure impairs sensorimotor gating and drives stereotypy

To test for lasting behavioral effects following in utero LSD exposure, we evaluated offspring at P90 on prepulse inhibition of acoustic startle (PPI, **Fig. 3A**) and open-field behavior.

Pregnant mice received either one single LSD injection at E12.5 (acute) or daily injections from E12.5 to E16.5 (repeated), with repeated saline-treated dams as controls (**Fig. 3B**).

When sexes were combined, PPI was reduced after prenatal LSD (**Fig. 3C**). In sex-stratified analyses, males showed reduced PPI following repeated exposure (**Fig. 3D**), whereas females did not differ at the group level at this N despite clear individual variability (**Fig. 3E**). Startle amplitude was higher in females across several LSD conditions across intensities (**Fig. 3H**), and in males differs only for the repeated group at the highest intensity (**Fig. 3G**). Startle latency showed no consistent group effect. The only reliable change was a slower response at 82 dB in acute LSD females (**Fig. S2A-C**). These patterns indicate that amplitude changes do not account for the PPI reduction, which was most robust in males.

Open field revealed a stereotypy-dominant phenotype rather than gross hyperactivity. Representative single-mouse occupancy heatmaps are shown in **Fig. 3H**, with group-mean occupancy heatmaps in **Fig. 3I**. Total rotations were increased following prenatal LSD (negative-binomial GLM, Group LR χ^2=8.02, P=0.018; back-transformed means ±SE: control 54.2 ±12.6, acute 136.2 ±31.3, repeated 81.4 ±18.8; Tukey control vs acute P=0.013; **Fig. 3J**). Using a control-anchored threshold (95th percentile of control), "high-rotators" were more frequent in LSD groups (acute 2/10, repeated 4/10, control 1/10; **Fig. 3K**). Spatial organization shifted without large changes in distance or velocity, as observed in pooled centroid distributions (**Fig. 3L**) and in the full set of raw path traces (**Fig. S2D**). Direction-specific rotation counts are provided in **Fig. S2E**.

Attempts to assess higher-order behaviors, including novel object recognition and social approach, were confounded by elevated baseline stereotypy and abnormal exploration, rendering these assays uninterpretable. Beginning at P21 and persisting through at least P156, 7 of 10 mice

with repeated exposure and 5 of 10 with acute exposure exhibited continuous stereotypies (backflipping, tight circling, upright corner-hopping). At P156, females had lower body weight following chronic exposure (35.3 vs 43.7 g, P=0.021) and higher brain mass after acute exposure (0.635 vs 0.550 g, P=0.0001); males did not differ, and the acute female brain-mass effect remained significant after adjusting for body weight (**Fig. S3A-H**). Testis mass was unchanged; the testis-to-body ratio was higher after acute exposure (P=0.021). A blinded midline screen of atlas-matched coronal sections at P156 identified ventriculomegaly with frontal-horn predominance in LSD groups (control 1/10, acute 9/10, repeated 8/10; **Fig. S3I**) and rarer callosal variants, including asymmetric hypoplasia, an occasional supracallosal diverticulum continuous with the frontal horn, and partial agenesis of the anterior corpus callosum; given limited atlas levels and modest N, these reads are descriptive.

Overall, prenatal LSD produced a coherent adult phenotype: male-biased deficits in sensorimotor gating, persistent stereotypy and rotational bias without generalized hyperactivity, and midline variants at P156. Considering the rapid appearance of LSD in embryonic CSF and the P8 cerebral cortical disruptions, these results show that a brief serotonergic exposure during E12.5–E16.5 is sufficient to durably alter circuit function and behavior, defining a discrete window of vulnerability with measurable anatomical and behavioral sequelae. Motivated by this window, we next asked which embryo-facing interface detects maternal psychedelics and initiates the early response.

Maternal psychedelics activate embryonic choroid plexus and change CSF

Given the rapid appearance of LSD in embryonic CSF and its effects on cortical development, we asked whether the embryonic ChP, a key interface for CSF production and

signaling, is an early target of maternal psychedelic exposure. Because the embryonic ChP expresses 5-HT_2C, we hypothesized that maternal serotonergic drugs directly activate ChP epithelial cells and trigger a secretory response (*12*, *13*). Pregnant dams received LSD (0.3 mg kg^{-1}), psilocybin (3 mg kg^{-1}), 5-MeO-DMT (50 mg kg^{-1}), or the 5-HT_2C agonist WAY-161503 (3 mg kg^{-1}) at E12.5; tissues and CSF were collected 30 min later (**Fig. 4A–B**).

A single maternal dose of LSD at E12.5 or E16.5 induced rapid activation of ChP epithelium across ventricles. The immediate early gene *Fos* was upregulated within 30 min, as measured by qPCR from microdissected ChP (adult lateral ventricle [LV] and E16.5 LV/third ventricle [3V]/fourth ventricle [4V]; **Fig. 4C–G**) and by c-FOS immunostaining (**Fig. 4B,H**). The response generalized to WAY-161503, 5-MeO-DMT, and psilocybin (**Fig. 4D–F,G**). Whole-head light-sheet imaging of optically cleared E12.5 embryos further confirmed robust c-FOS in 4V ChP with detectable, but less intense signal in LV ChP (**Fig. 4L, Fig. S4A-F**). Additional FOS signal was observed in the locus coeruleus in these datasets (anatomical observation; not quantified; **Fig. S4G–H**).

Downstream of transcriptional activation, ChP cells showed rapid apical remodeling. Within 30 min of maternal LSD, psilocybin, or 5-MeO-DMT, epithelial cells exhibited increased aposome formation (actin-rich, secretory protrusions [phalloidin/ezrin]), consistent with an apocrine-like secretory state (*14*, *15*) (**Fig. 4B,I,L,M**; **Fig. S5B-C**). Functionally, total protein concentration rose in embryonic CSF 30 min following maternal psychedelics at both E12.5 and E16.5 (**Fig. 4J–K**). Together, these data support that maternal psychedelic exposure activates embryonic ChP leading to rapid transcriptional, cytoskeletal, and secretory responses that alter CSF composition.

Discussion

This work reveals an embryo-facing detection system for maternal serotonergic drugs: minutes-scale access of LSD to embryonic CSF is sufficient to trigger a ChP response that shifts cerebral cortical assembly and imparts durable behavioral signatures.

The mechanism relaying maternal compounds to the developing offspring brain *in utero* is remarkably swift. Our pharmacokinetic data show that LSD appears in embryonic CSF as early as five minutes following maternal injection and peaking at approximately 15 minutes. This rapid ingress allows LSD to interact with targets on the ChP epithelium. Given that the 5-HT_2C receptor is the sole serotonin receptor subtype expressed in these cells, it represents the most likely target for this engagement. Coincident with LSD's appearance in the CSF, we observe a robust cellular response: rapid *Fos* upregulation, apical cytoskeletal remodeling consistent with apocrine secretion, and a functional increase in total CSF protein. By gaining access to this privileged compartment, exogenous agonists can immediately reshape the extracellular signals that pattern the developing cortex.

The consequences of this transient embryonic exposure are profound and permanent. A single maternal LSD dose was sufficient to disrupt cerebral cortical layering, while repeated dosing amplified these deficits with a pronounced male bias, shifting neuronal identity from upper-layer $SATB2^+$ to deep-layer $CTIP2^+$ cells and increasing microglial density. These structural disruptions, particularly the male-specific neuronal shifts, were paralleled by lasting functional impairments, including a deficit in prepulse inhibition that was statistically robust only in males. and a striking phenotype of spontaneous, rotational stereotypy. While this stereotypy confounded other cognitive assays, we contend it is a clinically significant finding, as pervasive, repetitive behaviors are a core

feature of neurodevelopmental disorders like autism, which also show a strong male prevalence (*16*).

Several limitations also warrant discussion. Importantly, our dosing strategy was chosen from established rodent literature to provide a robust signal for mechanistic discovery, aligning with doses that reliably engage 5-HT_2A-dependent behaviors (*17–19*), rather than via reverse translation from human use patterns. The doses applied remain well below the median lethal dose (*20*) and showed no overt maternal toxicity in our study. We observed no differences in dam weight, grooming, or pup retrieval and no birth-outcome changes, reducing the likelihood of postnatal care confounds. Nevertheless, while direct dose comparisons using mg kg^{-1} can pose substantial translational concerns across species, peripheral LSD concentrations observed here were approximately 100-fold higher than those observed following human exposure to LSD doses used in clinical trials (200 µg) (*21–23*). Therefore, future work should anchor translational efforts and dose selection with PK/PD and receptor-occupancy benchmarks. Additionally, while our data strongly implicate 5-HT_2C in the ChP, we cannot rule out parallel, direct actions of LSD on developing cortical neurons themselves. Future work is also needed to identify the specific CSF proteins responsible for the cortical phenotypes and to extend these findings to human-relevant models, accounting for interspecies differences in placental transport and neurodevelopmental timelines.

As psychedelics advance toward clinical application, amidst a landscape of expanding recreational use (*24–26*), our findings provide a critical, evidence-based foundation for assessing their neurodevelopmental risks. The data establish a new framework for understanding prenatal

drug exposures and underscore the need for caution and further research as these powerful serotonergic compounds become more widespread.

References

1. R. G. Dos Santos, J. C. Bouso, M. Á. Alcázar-Córcoles, J. E. C. Hallak, Efficacy, tolerability, and safety of serotonergic psychedelics for the management of mood, anxiety, and substance-use disorders: a systematic review of systematic reviews. *Expert Rev Clin Pharmacol* **11**, 889–902 (2018).

2. J. Calleja-Conde, J. A. Morales-García, V. Echeverry-Alzate, K. M. Bühler, E. Giné, J. A. López-Moreno, Classic psychedelics and alcohol use disorders: A systematic review of human and animal studies. *Addict Biol* **27**, e13229 (2022).

3. A. Carvajal-Oliveros, J. M. Campusano, Studying the Contribution of Serotonin to Neurodevelopmental Disorders. Can This Fly? *Front Behav Neurosci* **14**, 601449 (2021).

4. P. Gaspar, O. Cases, L. Maroteaux, THE DEVELOPMENTAL ROLE OF SEROTONIN : NEWS FROM MOUSE MOLECULAR GENETICS. *Nature Reviews Neuroscience* **4** (2003).

5. R. Shah, E. Courtiol, F. X. Castellanos, Abnormal Serotonin Levels During Perinatal Development Lead to Behavioral Deficits in Adulthood. *Frontiers in Behavioral Neuroscience* **12**, 1–10 (2018).

6. M. P. Lun, E. S. Monuki, M. K. Lehtinen, Development and functions of the choroid plexus-cerebrospinal fluid system. *Nat Rev Neurosci* **16**, 445–457 (2015).

7. N. Dani, R. H. Herbst, C. McCabe, G. S. Green, K. Kaiser, J. P. Head, J. Cui, F. B. Shipley, A. Jang, D. Dionne, L. Nguyen, C. Rodman, S. J. Riesenfeld, J. Prochazka, M. Prochazkova, R. Sedlacek, F. Zhang, V. Bryja, O. Rozenblatt-Rosen, N. Habib, A. Regev, M. K. Lehtinen, A cellular and spatial map of the choroid plexus across brain ventricles and ages. *Cell* **184**, 3056-3074.e21 (2021).

8. E. Vinsland, S. M. Salas, I. Kapustová, L. Hu, S. Webb, X. Li, X. He, M. Nilsson, M. Haniffa, R. Barker, O. Persson, D. R. Raleigh, E. Sundström, P. Lönnerberg, S. Linnarsson, Cell atlas of the developing human meninges reveals a dura origin of meningioma. bioRxiv [Preprint] (2025). https://doi.org/10.1101/2025.07.08.663122.

9. N. R. Saunders, K. M. Dziegielewska, R. M. Fame, M. K. Lehtinen, S. A. Liddelow, The choroid plexus: a missing link in our understanding of brain development and function. *Physiological Reviews* **103**, 919–956 (2023).

10. Y. Courtney, J. P. Head, N. Dani, O. V. Chechneva, F. B. Shipley, Y. Zhang, M. J. Holtzman, C. Sadegh, T. A. Libermann, M. K. Lehtinen, Choroid plexus apocrine secretion shapes CSF proteome during brain development. *Nature Neuroscience* (2025).

11. M. W. Zappaterra, A. S. LaMantia, C. A. Walsh, M. K. Lehtinen, Isolation of Cerebrospinal Fluid from Rodent Embryos for use with Dissected Cerebral Cortical Explants. *J Vis Exp*, 50333 (2013).

12. E. Sanders-Bush, M. Breeding, Choroid plexus epithelial cells in primary culture: a model of 5HT1C receptor activation by hallucinogenic drugs. *Psychopharmacology (Berl)* **105**, 340–346 (1991).

13. I. M. Diab, D. X. Freedman, L. J. Roth, [^{3} H]Lysergic Acid Diethylamide: Cellular Autoradiographic Localization in Rat Brain. *Science* **173**, 1022–1024 (1971).

14. Y. Courtney, J. P. Head, N. Dani, O. V. Chechneva, F. B. Shipley, Y. Zhang, M. J. Holtzman, C. Sadegh, T. A. Libermann, M. K. Lehtinen, Choroid plexus apocrine secretion shapes CSF proteome during mouse brain development. *Nat Neurosci*, 1–14 (2025).

15. Y. Courtney, M. K. Lehtinen, Apocrine secretion by the choroid plexus. *Fluids and Barriers of the CNS* **22**, 75 (2025).

16. T. May, I. Adesina, J. McGillivray, N. J. Rinehart, Sex differences in neurodevelopmental disorders. *Curr Opin Neurol* **32**, 622–626 (2019).

17. A. L. Halberstadt, M. A. Geyer, Characterization of the head-twitch response induced by hallucinogens in mice: detection of the behavior based on the dynamics of head movement. *Psychopharmacology (Berl)* **227**, 10.1007/s00213-013-3006-z (2013).

18. S. A. McGriff, J. C. Hecker, A. D. Maitland, J. S. Partilla, M. H. Baumann, G. C. Glatfelter, Psychedelic-like effects induced by 2,5-dimethoxy-4-iodoamphetamine, lysergic acid diethylamide, and psilocybin in male and female C57BL/6J mice. *Psychopharmacology*, doi: 10.1007/s00213-025-06795-x (2025).

19. A. D. Maitland, N. R. Gonzalez, D. Walther, F. Pereira, M. H. Baumann, G. C. Glatfelter, Rapid, Open-Source, and Automated Quantification of the Head Twitch Response in C57BL/6J Mice Using DeepLabCut and Simple Behavioral Analysis. *ACS Pharmacol. Transl. Sci.* **8**, 2694–2709 (2025).

20. L. A. Henríquez-Hernández, J. Rojas-Hernández, D. J. Quintana-Hernández, L. F. Borkel, Hofmann vs. Paracelsus: Do Psychedelics Defy the Basics of Toxicology?—A Systematic Review of the Main Ergolamines, Simple Tryptamines, and Phenylethylamines. *Toxics* **11**, 148 (2023).

21. F. Holze, P. Gasser, F. Müller, P. C. Dolder, M. E. Liechti, Lysergic Acid Diethylamide–Assisted Therapy in Patients With Anxiety With and Without a Life-Threatening Illness: A Randomized, Double-Blind, Placebo-Controlled Phase II Study. *Biological Psychiatry* **93**, 215–223 (2023).

22. P. C. Dolder, Y. Schmid, A. E. Steuer, T. Kraemer, K. M. Rentsch, F. Hammann, M. E. Liechti, Pharmacokinetics and Pharmacodynamics of Lysergic Acid Diethylamide in Healthy Subjects. *Clin Pharmacokinet* **56**, 1219–1230 (2017).

23. P. C. Dolder, Y. Schmid, M. Haschke, K. M. Rentsch, M. E. Liechti, Pharmacokinetics and Concentration-Effect Relationship of Oral LSD in Humans. *Int J Neuropsychopharmacol* **19**, pyv072 (2016).

24. K. M. Rockhill, J. C. Black, M. S. Ladka, K. B. Sumbundu, H. A. Olsen, J. S. Jewell, J. Hunt, R. C. Wolf, K. Nerurkar, R. C. Dart, A. A. Monte, The Rise of Psilocybin Use in the United States: A Multisource Observational Study. *Ann Intern Med* **178**, 1052–1054 (2025).

25. M. E. Patrick, R. A. Miech, L. D. Johnston, P. M. O'Malley, "Monitoring the Future Panel Study annual report: National data on substance use among adults ages 19 to 65, 1976–2023" (Institute for Social Research, 2024); https://doi.org/10.7826/ISR-UM.06.585140.002.07.0003.2024.

26. O. Livne, D. Shmulewitz, C. Walsh, D. S. Hasin, Adolescent and adult time trends in US hallucinogen use, 2002–19: any use, and use of ecstasy, LSD and PCP. *Addiction* **117**, 3099–3109 (2022).

Acknowledgments: We thank the NIDA Drug Supply Program for providing controlled substances (LSD, psilocybin, and 5-MeO-DMT) used in this study. We are grateful to Chinfei Chen, Hisashi Umemori, and Harry Cramer for imaging advice and support, and to the BCH IDDRC Cellular Imaging Core (RRID: SCR_026485) for confocal and light sheet imaging. We are especially grateful to the Boston Children's Hospital Research Controlled Substances Team for their guidance throughout this project. We thank Nathaniel Hodgson and the BCH Animal Behavior and Physiology Core for assistance with behavioral assays. We thank Sofia Bennetts for technical support and help with figures. We are grateful to syGlass (SyGlass, Inc.) for extended access to their visualization software under a trial license and for technical assistance. syGlass had no role in study design, data collection, data analysis, or the decision to publish. Figures were created in part using BioRender.com. We thank members of the Lehtinen lab for valuable feedback and discussions.

Funding:

National Institutes of Health grant R01NS088566 (MKL)

National Institutes of Health grant P50HD105351 (BCH IDDRC)

National Institutes of Health grant S10OD030322 (BCH IDDRC)

Howard Hughes Medical Institute Gilliam Fellowship (YC)

The Jane Coffin Childs Memorial Fund for Medical Research Fellowship (YC)

Kirby Innovation Award (MKL)

Author contributions:

Conceptualization: YC.
Methodology: YC, JMA.
Investigation: YC, JMA, CLL.
Visualization: YC, JMA.
Funding acquisition: YC, CJW, MKL.

Project administration: CJW, MKL.

Supervision: CJW, MKL.

Writing – original draft: YC.

Writing – review & editing: YC, JMA, CLL, CJW, MKL.

Competing interests: Authors declare that they have no competing interests.

Data and materials availability: All data needed to evaluate the conclusions of this study are present in the paper and/or the Supplementary Materials. Additional data and analysis scripts are available from the corresponding author upon reasonable request. Controlled substances (LSD, psilocybin, 5-MeO-DMT) were obtained from the NIDA Drug Supply Program and cannot be redistributed; qualified investigators should request these materials directly from NIDA.

Supplementary Materials

Materials and Methods

Supplementary Text

Figs. S1 to S4

Tables S1 to S2

References (27-34)

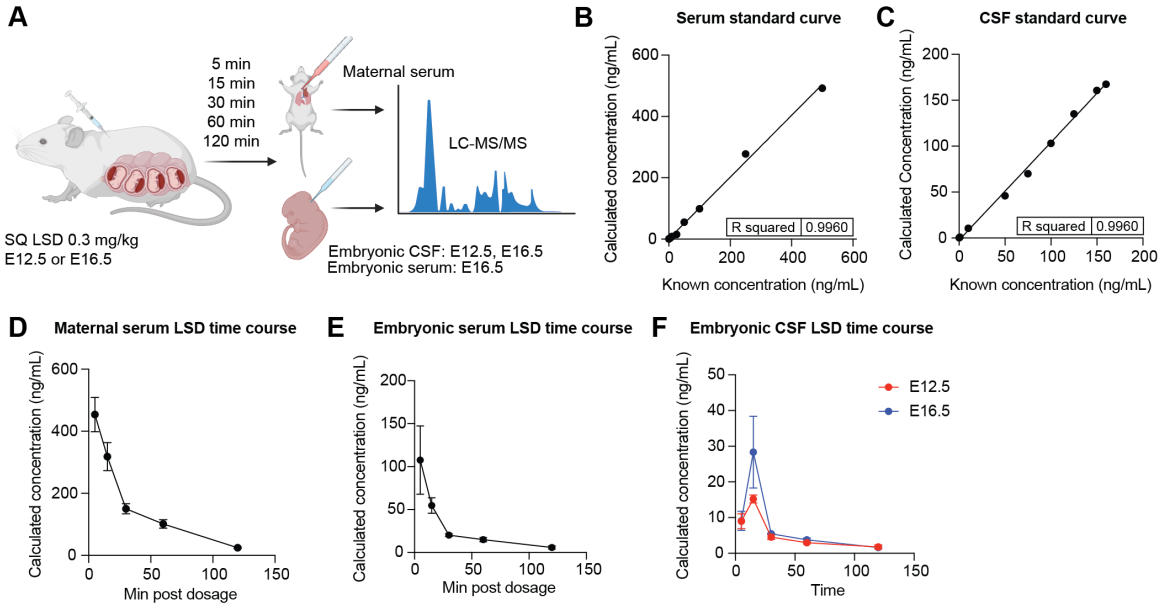

Fig. 1. Maternal LSD rapidly enters embryonic circulation and CSF. (A) Schematic of the pharmacokinetic study. Pregnant mice received a single subcutaneous injection of LSD (0.3 mg kg^{-1}) at E12 .5 or E16.5. Maternal serum, embryonic serum (E16.5) and embryonic CSF (E12.5, E16.5) were sampled at 5, 15, 30, 60, and 120 min and analyzed by LC-MS/MS. **(B)** Calibration curve for LSD spiked into serum ($R^2 = 0.996$). **(C)** Calibration curve for LSD spiked into CSF ($R^2 = 0.996$). **(D)** Time course of LSD concentration in maternal serum after 0.3 mg kg^{-1} LSD (mean ± SEM, n = 3 dams per time point). **(E)** Time course of LSD concentration in E16.5 serum after 0.3 mg kg^{-1} maternal LSD (mean ± SEM, n = 3 pooled litters per time point). **(F)** LSD concentration in embryonic CSF at E12 .5 or E16.5 peaks at 15 min then declines yet remains detectable at 120 min (mean ± SEM, n = 3 pooled litters per time point).

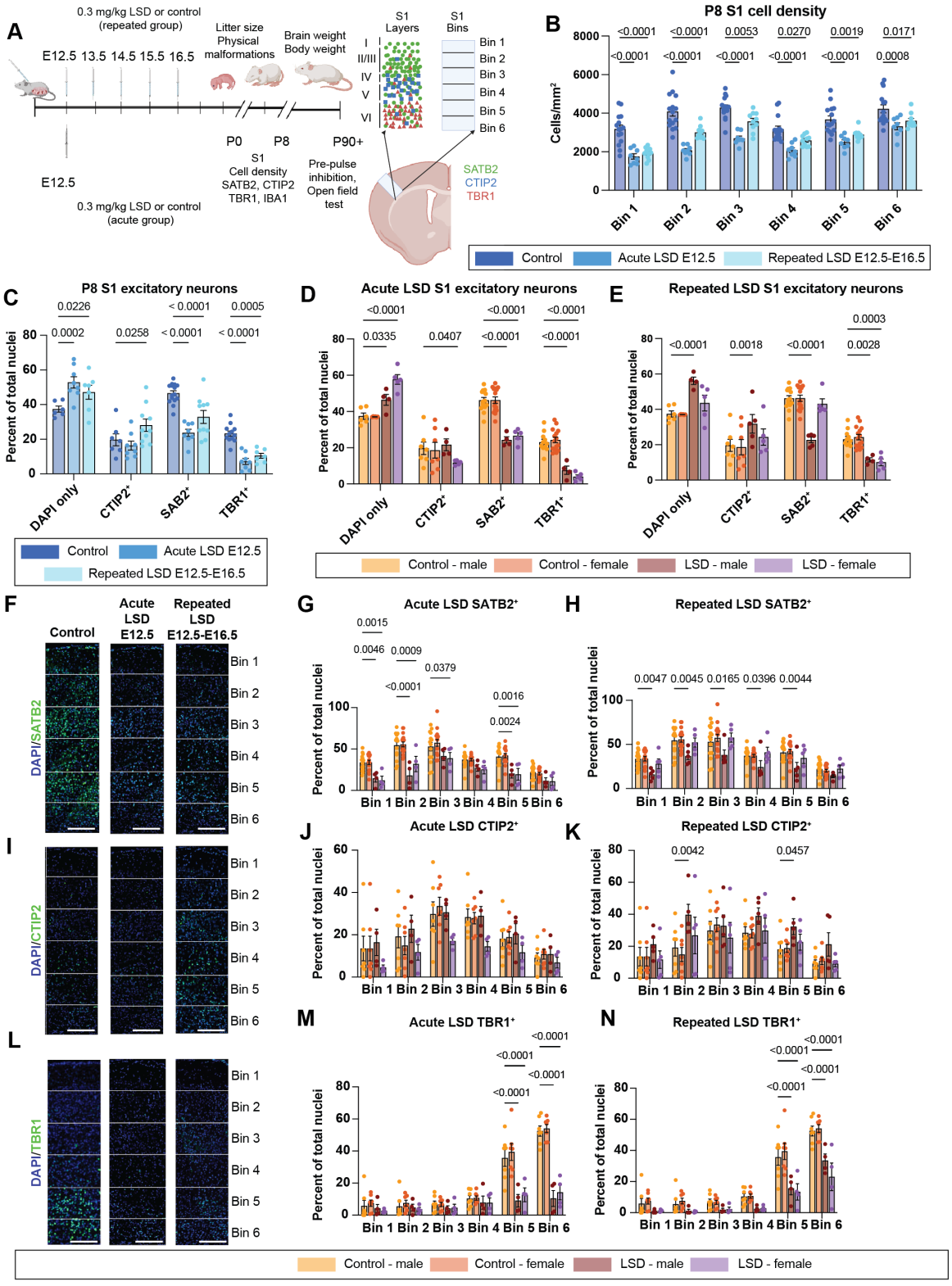
A
0.3 mg/kg LSD or control (repeated group)
E12.5 13.5 14.5 15.5 16.5
Litter size
Physical malformations
Brain weight
Body weight
S1 Layers
S1 Bins
I
II/III
IV
V
VI
Bin 1
Bin 2
Bin 3
Bin 4
Bin 5
Bin 6
P0
P8
P90+
E12.5
S1
Cell density
SATB2, CTIP2
TBR1, IBA1
Pre-pulse inhibition, Open field test
SATB2
CTIP2
TBR1
0.3 mg/kg LSD or control (acute group)
B
P8 S1 cell density
Cells/mm²
Control
Acute LSD E12.5
Repeated LSD E12.5-E16.5
C
P8 S1 excitatory neurons
Percent of total nuclei
DAPI only
CTIP2⁺
SAB2⁺
TBR1⁺
D
Acute LSD S1 excitatory neurons
E
Repeated LSD S1 excitatory neurons
Control - male
Control - female
LSD - male
LSD - female
F
Control
Acute LSD E12.5
Repeated LSD E12.5-E16.5
DAPI/SATB2
G
Acute LSD SATB2⁺
H
Repeated LSD SATB2⁺
I
DAPI/CTIP2
J
Acute LSD CTIP2⁺
K
Repeated LSD CTIP2⁺
L
DAPI/TBR1
M
Acute LSD TBR1⁺
N
Repeated LSD TBR1⁺
O
Hoechst/IBA1
100 µm
IBA1⁺ cells/mm²

Fig. 2. Prenatal LSD alters S1 cortical composition with dose- and sex-contingent effects. (A) Experimental design and S1 sampling. Pregnant dams received a single LSD dose at E12.5 ("acute") or daily doses at E12.5–E16.5 ("repeated") at 0.3 mg kg^{-1}. Brains were analyzed at P8. S1 was divided into six equal-width bins from pia (Bin 1) to white matter (Bin 6). **(B)** Total cell density ($DAPI^+$ nuclei mm^{-2}) across depth. Both regimens reduce nuclei relative to controls; exact post hoc *P* values are printed above bins. **(C)** Sexes pooled: composition of excitatory-layer markers expressed as percent of total nuclei (DAPI-only, $CTIP2^+$, $SATB2^+$, $TBR1^+$). Repeated exposure increases $CTIP2^+$ and decreases $SATB2^+/TBR1^+$; acute exposure decreases $SATB2^+/TBR1^+$ without increasing $CTIP2^+$ (panel *P* values shown). **(D–E)** Sex-stratified marker composition for acute (**D**) and repeated (**E**) exposure (color key indicates sex and treatment). **(F)** Representative S1 micrographs (male) stained for SATB2 (green) with DAPI (blue). Scale bar, 50 µm. **(G–H)** $SATB2^+$ neurons by depth after acute (**G**) or repeated (**H**) exposure (percent of total nuclei per bin). Male-biased reductions are evident across superficial to mid layers; bin-wise *P* values are printed. **(I)** Representative S1 micrographs (male) stained for CTIP2 (green) with DAPI (blue). Scale bar, 50 µm. **(J–K)** $CTIP2^+$ neurons by depth after acute (**J**) or repeated (**K**) exposure. Repeated exposure produces bin-restricted increases in males (bin-wise *P* values shown). **(L)** Representative S1 micrographs (male) stained for TBR1 (green) with DAPI (blue). Scale bar, 50 µm. **(M–N)** $TBR1^+$ neurons by depth after acute (**M**) or repeated (**N**) exposure, showing deep-layer losses in both sexes (bin-wise *P* values shown). **(O)** $IBA1^+$ microglia: representative images (scale bars, 100 µm) and density quantification (cells mm^{-2}). Microglia density increases with repeated exposure and is modestly elevated after acute exposure (exact *P* values on panel). **Imaging note (F, I, L):** Confocal micrographs are mosaics of adjacent fields stitched with linear blending. Quantification was performed on the original high-resolution tiles (identical acquisition settings across groups), excluding seam margins; minor stitch seams may be visible.

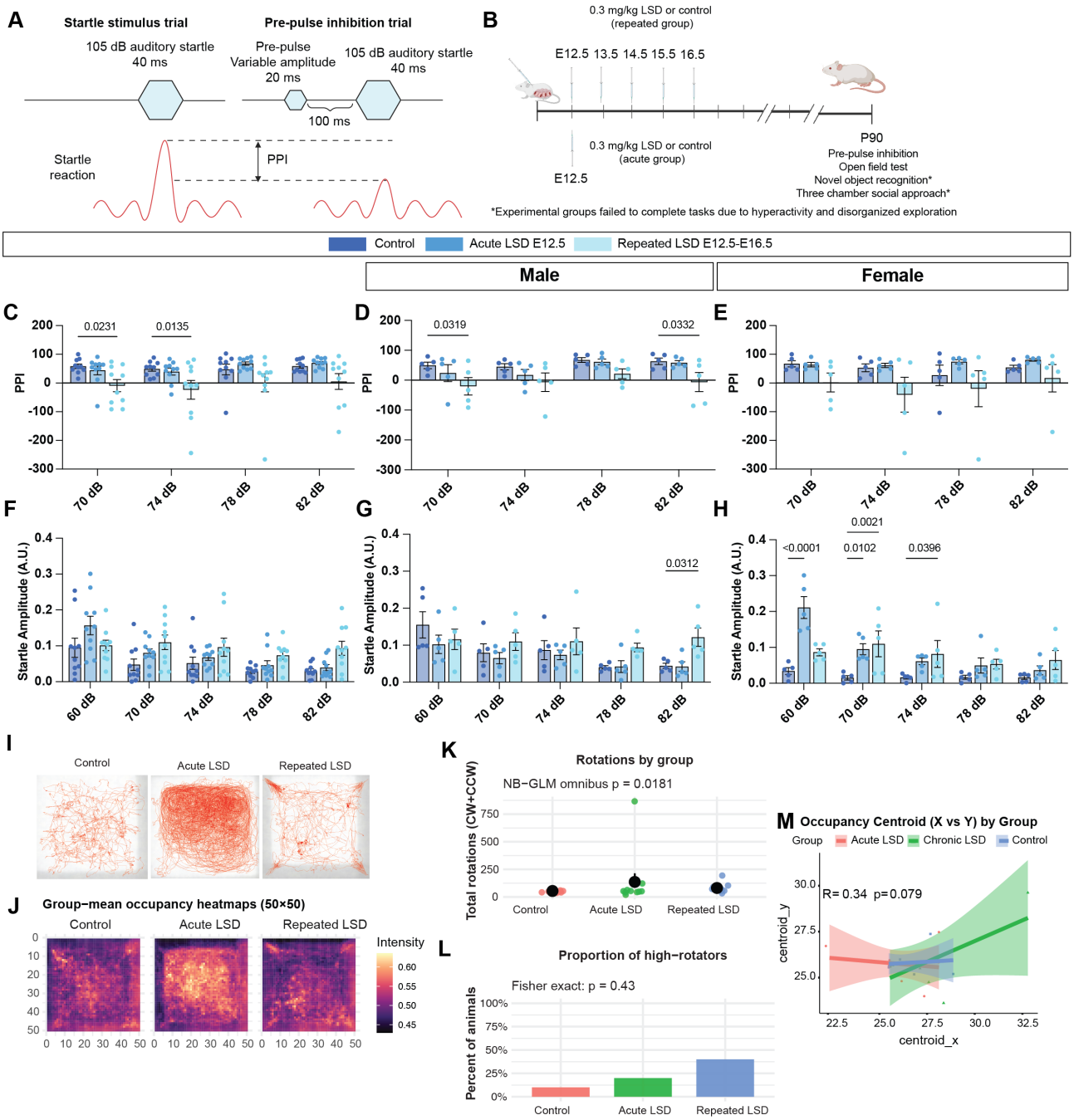
A
Startle stimulus trial
105 dB auditory startle
40 ms
Pre-pulse inhibition trial
Pre-pulse
Variable amplitude
20 ms
105 dB auditory startle
40 ms
100 ms
Startle
reaction
PPI
B
0.3 mg/kg LSD or control
(repeated group)
E12.5 13.5 14.5 15.5 16.5
0.3 mg/kg LSD or control
(acute group)
E12.5
P90
Pre-pulse inhibition
Open field test
Novel object recognition*
Three chamber social approach*
*Experimental groups failed to complete tasks due to hyperactivity and disorganized exploration
Control
Acute LSD E12.5
Repeated LSD E12.5-E16.5
Male
Female
C
D
E
PPI
0.0231
0.0135
0.0319
0.0332
70 dB
74 dB
78 dB
82 dB
F
G
H
Startle Amplitude (A.U.)
0.0312
<0.0001
0.0102
0.0021
0.0396
60 dB
70 dB
74 dB
78 dB
82 dB
I
Control
Acute LSD
Repeated LSD
J
Group−mean occupancy heatmaps (50×50)
Control
Acute LSD
Repeated LSD
Intensity
K
Rotations by group
NB−GLM omnibus p = 0.0181
Total rotations (CW+CCW)
Control
Acute LSD
Repeated LSD
L
Proportion of high−rotators
Fisher exact: p = 0.43
Percent of animals
M
Occupancy Centroid (X vs Y) by Group
Group
Acute LSD
Chronic LSD
Control
R= 0.34 p=0.079
centroid_y
centroid_x

Fig. 3. Embryonic LSD exposure impairs sensorimotor gating and increases rotational stereotypy. Analyses were blinded; litter was tracked and included as a random intercept in sensitivity models. **(A)** PPI task schematic. **(B)** Maternal dosing and testing timeline (acute E12.5; repeated E12.5–E16.5; saline controls). **(C–E)** Prepulse inhibition (PPI) at P90: **(C)** sexes pooled, PPI reduced after prenatal LSD; **(D)** males, reduced PPI after repeated exposure; **(E)** females, no group-level difference at this N despite individual variability. **(F–H)** Startle amplitude across intensities (A.U.): **(F)** sexes pooled; **(G)** males, higher amplitude only for the repeated group at 82 dB; **(H)** females, higher amplitude in several LSD conditions across intensities. **(I)** Open-field examples: single-animal path traces. **(J)** Group-mean occupancy heatmaps (50×50 grid). **(K)** Total rotations by group (negative-binomial GLM, omnibus $\chi^2 = 8.02$, $P = 0.018$); back-transformed means ± SE: Control 54.2 ± 12.6, Acute 136.2 ± 31.3, Repeated 81.4 ± 18.8; Tukey Control vs Acute $P = 0.013$. **(L)** Proportion of "high-rotators" (threshold = 95th percentile of Control; Fisher exact $P = 0.43$; n/N shown). **(M)** Occupancy centroids (x by y), sexes pooled; lines show group-wise linear fits with 95% confidence bands ($R = 0.34$, $P = 0.079$).

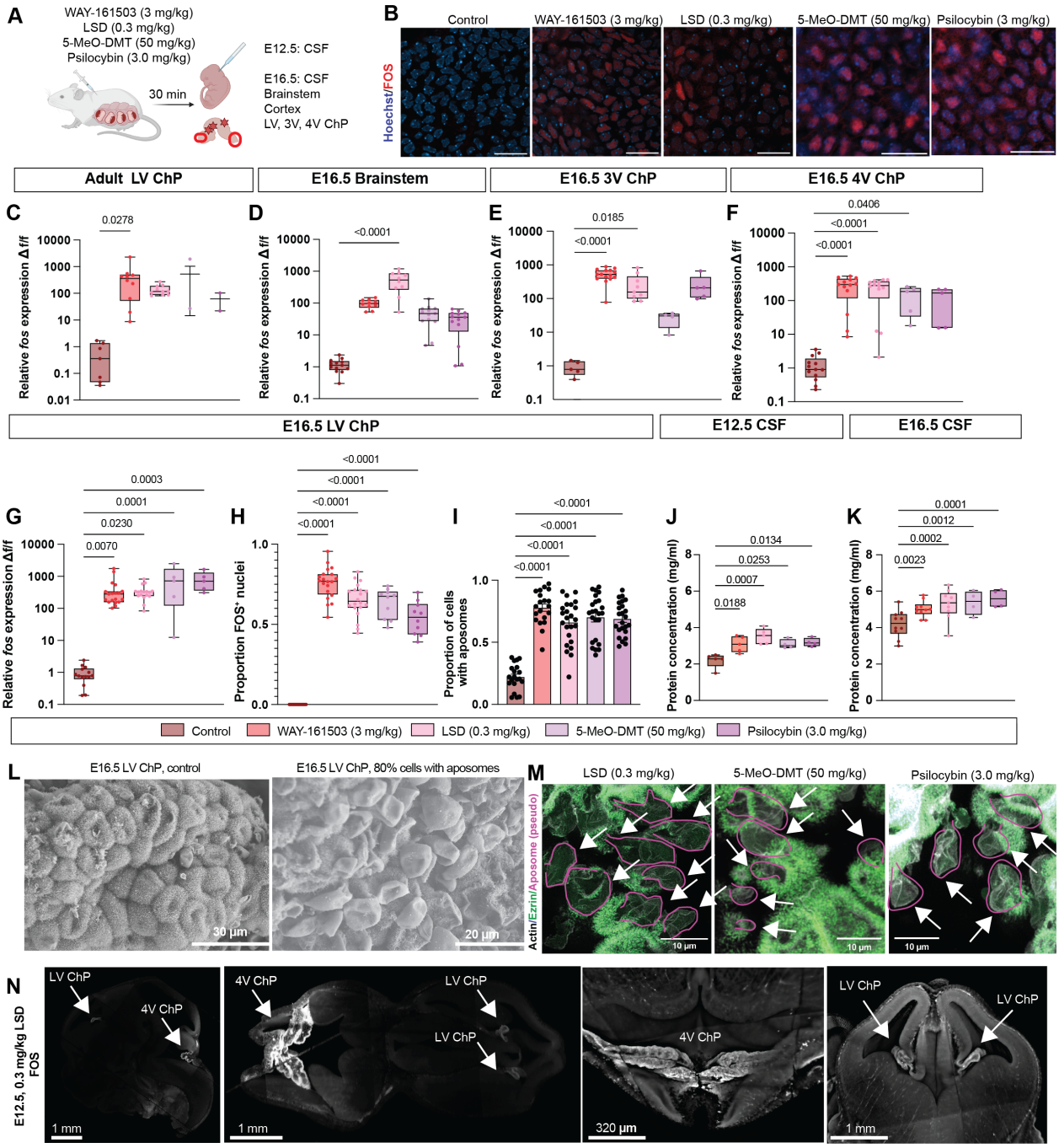
A
WAY-161503 (3 mg/kg)
LSD (0.3 mg/kg)
5-MeO-DMT (50 mg/kg)
Psilocybin (3.0 mg/kg)
30 min
E12.5: CSF
E16.5: CSF
Brainstem
Cortex
LV, 3V, 4V ChP
B
Control
WAY-161503 (3 mg/kg)
LSD (0.3 mg/kg)
5-MeO-DMT (50 mg/kg)
Psilocybin (3 mg/kg)
Hoechst/FOS
Adult LV ChP
E16.5 Brainstem
E16.5 3V ChP
E16.5 4V ChP
C
D
E
F
Relative fos expression Δ f/f
E16.5 LV ChP
E12.5 CSF
E16.5 CSF
G
H
I
J
K
Proportion FOS+ nuclei
Proportion of cells with aposomes
Protein concentration (mg/ml)
Control
WAY-161503 (3 mg/kg)
LSD (0.3 mg/kg)
5-MeO-DMT (50 mg/kg)
Psilocybin (3.0 mg/kg)
L
E16.5 LV ChP, control
E16.5 LV ChP, 80% cells with aposomes
30 µm
20 µm
M
LSD (0.3 mg/kg)
5-MeO-DMT (50 mg/kg)
Psilocybin (3.0 mg/kg)
Actin/Ezrin/Aposome (pseudo)
10 µm
N
E12.5, 0.3 mg/kg LSD
FOS
LV ChP
4V ChP
1 mm
320 µm

Fig. 4. Maternal psychedelics induce a 5-HT$_2$C agonist-like secretory response in the embryonic choroid plexus. (A) Experimental design: pregnant dams dosed at E12.5 (LSD 0.3 mg kg^{-1}; 5-MeO-DMT 50 mg kg^{-1}; psilocybin 3 mg kg^{-1}; WAY-161503 3 mg kg^{-1}); tissues and CSF collected 30 min later. Additional cohorts at E16.5 as indicated. **(B)** c-FOS immunostaining in ChP epithelium 30 min post-dose (representative fields; Hoechst/c-FOS). **(C)** Adult LV ChP: Fos qPCR (ΔΔ). **(D–F)** E16.5 ChP/brainstem: Fos qPCR (ΔΔ) in **D**, brainstem; **E**, 3V ChP; **F**, 4V ChP. **(G)** E16.5 LV ChP: Fos qPCR (ΔΔ). **(H)** Proportion of FOS$^+$ nuclei in E16.5 4V ChP (image-based quantification). **(I)** Proportion of ChP epithelial cells with apocrine blebs at 30 min. **(J–K)** Total protein concentration in embryonic CSF: **J**, E12.5; **K**, E16.5. (**L**) SEM of E16.5 LV choroid plexus comparing baseline aposome formation (left) with a high-frequency state (right; ~80% aposome-positive epithelial cells). (**M**) High-resolution confocal images of E16.5 ChP epithelium 30 min after LSD, 5-MeO-DMT, or psilocybin exposure shows extensive apical blebbing and redistribution of actin and ezrin, a marker of microvilli and membrane curvature. **(N)** Light-sheet fluorescence imaging of optically cleared E12.5 heads stained for c-FOS 30 min post maternal 0.3 mg kg^{-1} LSD (representative embryo). Cross-sections of whole-head dataset highlight strong activation in 4V ChP and detectable signal in LV ChP (arrows). Scattered bright foci are non-cellular artifacts (e.g., vascular-associated antibody retention and secondary antibody pooling) characteristic of this non-perfused, whole-embryo staining method. Scale bars as indicated.